

Tungsten oxide nanostructures growth in HFCVD system by slow positron beam

J. Lou^{1,a}, B.J. Ye¹, X.P. Wang², H.M. Weng¹, H.J. Du¹, Z.B. Zhang¹

¹Department of modern Physics, University of Science and Technology of China, Hefei 230026, P. R. China

²Department of Physics, University of Puerto Rico, P.O. Box 23343, San Juan, PR 00931, USA

^aemail: lou7502@mail.ustc.edu.cn

Keywords: tungsten oxide, nanostructure, nanobunlde, HFCVD, slow positron

Abstract: Tungsten oxide (WO_x) nanostructures were prepared by a hot filament chemical vapor deposition (HFCVD) system. Two series of samples were synthesized by adjusting filaments temperature (T_f) and oxygen gas concentration (OGC). The crystallinity and stoichiometry were highly related to T_f and OGC. The evolution of stoichiometry and types of defects was illuminated by slow positron implantation spectroscopy (SPIS). A turning point of $T_f=1750^\circ\text{C}$ was found that at this point the crystallinity and stoichiometry natures were the best. In order to develop the chemical phase from substoichiometric to stoichiometric, the oxygen gas concentration in the mixture gas during deposition should be raised to an appropriate level.

Introduction

Tungsten oxide materials has attracted much attention for its excellent electrochromic and photochromic properties and shows giant potentials for switchable windows [1], catalysts [2], lithium batteries [3] and electrochromic materials [4]. Recently, nanostructured tungsten oxide has been focused on gas sensors due to properties of high surface-to-volume ratio, high sensitivity, fast response time and room temperature operation [5]. In this report, tungsten oxide (WO_x) films were prepared by a HFCVD system which is simple, cheap, catalyst free and repeatable [6]. To prepare a series of samples, the temperature of the hot tungsten filaments were varied from 1550°C to 2100°C . Another series of samples were prepared with different OGC. Slow positron beam system was employed to characterize the influence of deposit conditions on as-prepared samples.

Experimental details

The tungsten oxide nanostructures were prepared by a HFCVD system. In first series of experiments, the chamber was first pumped to 3.5×10^{-2} Torr after placing the polished Si (100) substrates. Then, high purity argon gas was fed into the chamber. The gas pressure inside the chamber was maintained at 0.8 Torr and the flow rate of argon gas was 5sccm. The hot tungsten filaments temperature was monitored by an infrared ray pyrometer during the deposition for 30 min. In a series of experiments, the oxygen level was same, but T_f was maintained at different points that were 1550, 1650, 1750, 1900 and 2100°C for samples 1#, a# (only 10min deposition), 2#, 3# and 4#, respectively. The factors directly work on the growth of tungsten oxide nanostructures such as the tungsten oxide species saturation near the substrate, substrate temperature and temperature gradient between the hot filaments and substrates were all determined by the filament temperature T_f [7].

Another major factor was the deposition gas in the chamber. So in second series of experiments, oxygen gas concentration in the mixture gas was maintained at different levels by another HFCVD system. The Molybdenum (Mo) wafer was used as deposition substrate. After placing the substrate, the chamber was pumped down to 2.0×10^{-5} Torr. Three kinds of gas mixture, 8.7% of CH_4 , 0.3% of O_2 , 91% of H_2 (l-OGC); 8.5% of CH_4 , 0.5% of O_2 , 91% of H_2 (m-OGC) and 8.3% of CH_4 , 0.7% of O_2 , 91% of H_2 (h-OGC) gases were used. The flow rate of mixed gas was 5sccm. The gas pressure inside the chamber was maintained at 0.5 Torr and $T_f=2400^\circ\text{C}$ during the

deposition for 60 min. The deposition might be explained by the vapour-solid (VS) model [8].

Results and discussion

The samples were analyzed using a slow positron beam device. The S-E curves, fit performed by the program package VEPFIT, are presented in Fig.1. According to the formula of the mean depth $\langle z \rangle = (36 \times E^{1.62})/\rho$, the mean depth is between about 600nm (pure WO_3 films) to 200nm (pure α -W materials). The positron implantation profile at a given energy extends about twice the value of $\langle z \rangle$ [9]. All of the films are thicker than 1200nm by SEM (not shown), and almost no positrons annihilate in the Si substrates. Fig.1 (a) shows the measured S value of all samples first continuously decreases with the increase of positron energy and reaches a plateau value, which means the positrons were annihilated exclusively in the tungsten oxide films. When $T_f=1550$ and 1650°C , the plateau value of S is largest and decreases to the least at $T_f=1750^\circ\text{C}$. The plateau value of S increases when $T_f=1900$ and 2100°C . The content of low valence states W in samples a# is largest and samples 3# and 4# take second place. When low valence states W exist in the film, the free valence electrons that not form W-O bond around nucleus are still in existence because of the lack of oxygen. It is easier to be the effective positrons capture centers around low valence states W ions that increase S value. And the bound energies of valence electrons of stoichiometric W^{6+} are distinctly higher than that of low valence states of W [10]. S value is lowest when films are dominated by stoichiometric W^{6+} or WO_3 . The results of S-E curves coincide with that of XPS, namely S value coincides with the component ratio of stoichiometric W^{6+} that presented in fig.1 (b). The L_{eff} of samples 3# and 4# presented in fig.1 (c) are 8.59 ± 1.18 and $6.57 \pm 0.50\text{nm}$ respectively, illuminating the highly defected films present lots of vacancy agglomerates.

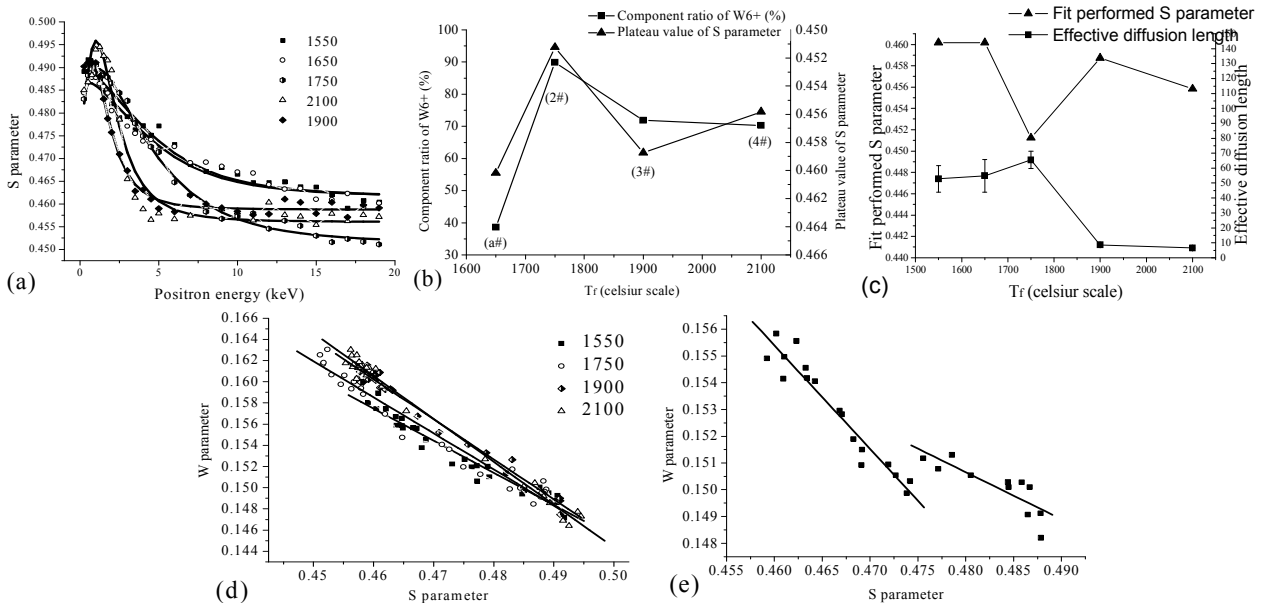


FIG1. Results of SPIS for first series of samples. (a) S parameter versus positron energy of samples. (b) Component ratio of stoichiometric W^{6+} calculated XPS results by and plateau value of S versus T_f of samples a#, 2#, 3# and 4#. (c) Fit performed S parameter and effective diffusion length of positrons of all samples. (d) S-W plots for samples 1#, 2#, 3# and 4#. (e) S-W plot for sample a#.

The variation of types of defects is revealed by S-W plots presented in fig.1 (d) and fig.1 (e). As shown in fig.1 (d), S-W points would be on one straight line if only one type of defects exist in the materials. The fitted straight lines of the samples slope with the increasing of T_f gradually (slope = -0.30307, -0.34087, -0.37824, -0.40473 for $T_f = 1550, 1750, 1900, 2100^\circ\text{C}$ respectively), which indicates the concentration of oxygen vacancies increased with T_f . Oxygen vacancies are not the positron capture centers, but can scatter positrons that decreases the diffusing length. The S-W plot of sample a#, only 10min deposited, is presented in fig.1 (e), which is different from other samples. There is no straight line between S-W points, which suggests a different surface layer about 30nm was synthesized. SPIS illuminates that the crystallinity and stoichiometry natures are best and the

defect concentration is lowest at the turning point $T_f = 1750^\circ \text{C}$ because of the minimal plateau value of S and maximal L_{eff} .

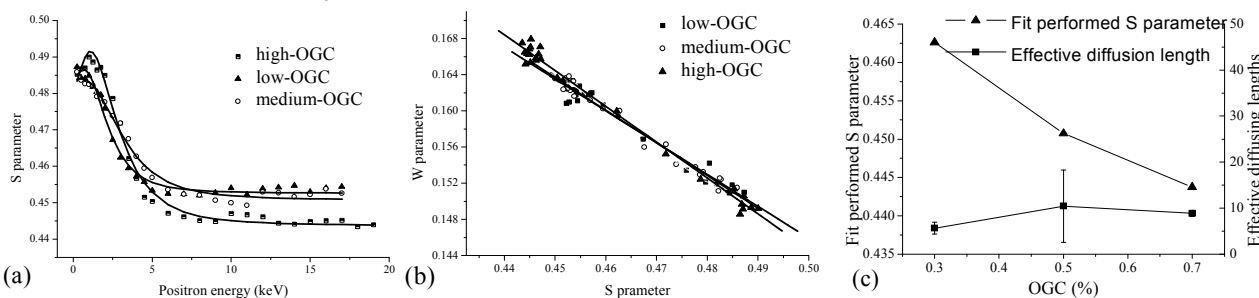


FIG.2 Results of SPIS for second series of samples. (a) S-E curves of samples at different OGC. (b) S-W plots for samples at different OGC. (c) Fit performed S parameter and effective diffusing lengths of positrons of samples at difference OGC.

The S-E curves and S-W plots for samples l-OGC, m-OGC and h-OGC are presented in fig.2. The plateau value of S of sample h-OGC is lowest, and that of sample l-OGC is largest. The plateau value of S decreases with the increase of OGC, which also coincide the fact that the rise of OGC from 0.3% to 0.7%, the chemical phase developed from substoichiometry to stoichiometry [11]. S-W plots show that the fitted straight lines of the samples slope with the decrease of OGC gradually (slope = -0.35232, -0.3616, and -0.39618 for L-OGC, M-OGC and H-OGC respectively), which indicates the concentration of oxygen vacancies increased with OGC.

Conclusions

Two series of tungsten oxide films were prepared by HFCVD at different T_f and OGC. A turning point was found that the crystallinity and stoichiometry natures were the best and the defect concentration was lowest. As T_f increased continuously, the film crystallinity decreased, correspondingly the component ratio of stoichiometry WO_3 decreased and lots of vacancy agglomerates presented. The chemical phase developed from substoichiometry to stoichiometry as the oxygen gas concentration in the mixture gas during deposition was raised to an appropriate level. Slow positron beam system is an effective and sensitive implement to identify the properties of stoichiometry and types of defects with depth of tungsten oxide thin films. In conclusion, T_f and OGC highly influence the properties of deposited tungsten oxide films and nanostructures. The properties of tungsten oxide can be controlled by adjusting the deposition parameters.

Acknowledgment

This work was supported by the National Nature Science Foundation of China (No.10675114 and 10675115).

References

- [1] A. Georg et al, vacuum **82**, 730 (2008)
- [2] M. Ponzi, C. Duschatzky, A. Carrascull, E. Ponzi, Appl. Catal. A **169**, 373 (1998)
- [3] A. Yu, M. Kumagai, Z. Liu, and J. Y. Lee, J. Solid State Electronchem. **2**, 394 (1998)
- [4] S. J. Yoo, J. W. Lim, Y. E. Sung, Appl. Phys. Lett. **90**, 173126 (2007)
- [5] Y. S. Kim et al, Appl. Phys. Lett. **86**, 213105 (2005)
- [6] N. Shankar, M. F. Yu, S. P. Vanka, N. G. Glumac, Mater. Lett. **60**, 771 (2006)
- [7] L. F. Chi et al, Nanotechnology **17**, 5590 (2006)
- [8] J. Zhou, N. S. Deng, J. Chen, J. C. She and Z. L. Wang, Adv. Mater. **15**, 1835 (2003)
- [9] G. Brauer et al, Nanotechnology **18**, 195301 (2007)
- [10] C. X. Ma, C. L. Zhou, M.Z. Zhang et al, Volume: **445-6**, 141 (2004)
- [11] X. P. Wang, B. Q. Yang, H. X. Zhang, and P. X. Feng, Nanoscale Res. Lett. **2**, 405 (2007)

Positron and Positronium Chemistry

doi:10.4028/0-87849-348-4

Tungsten Oxide Nanostructures Growth in HFCVD System by Slow Positron Beam

doi:10.4028/0-87849-348-4.195